

UC Davis

UC Davis Previously Published Works

Title

Brain oxylipin concentrations following hypercapnia/ischemia: effects of brain dissection and dissection time[S]

Permalink

<https://escholarship.org/uc/item/3b31c5dg>

Journal

Journal of Lipid Research, 60(3)

ISSN

0022-2275

Authors

Hennebelle, Marie
Metherel, Adam H
Kitson, Alex P
[et al.](#)

Publication Date

2019-03-01

DOI

10.1194/jlr.d084228

Peer reviewed



Brain oxylipin concentrations following hypercapnia/ischemia: effects of brain dissection and dissection time^S

Marie Hennebelle,* Adam H. Metherel,[†] Alex P. Kitson,[†] Yurika Otoki,^{**§} Jun Yang,^{**††} Kin Sing Stephen Lee,^{**††} Bruce D. Hammock,^{**††} Richard P. Bazinet,[†] and Ameer Y. Taha^{1,*}

Departments of Food Science and Technology* and Entomology and Nematology,** College of Agriculture and Environmental Sciences, and Comprehensive Cancer Center,^{††} University of California, Davis, Davis, CA; Department of Nutritional Sciences,[†] Faculty of Medicine, University of Toronto, Toronto, ON, Canada; and Food and Biodynamic Laboratory,[§] Graduate School of Agricultural Science, Tohoku University, Sendai, Japan

Abstract PUFAs are precursors to bioactive oxylipin metabolites that increase in the brain following CO₂-induced hypercapnia/ischemia. It is not known whether the brain-dissection process and its duration also alter these metabolites. We applied CO₂ with or without head-focused microwave fixation for 2 min to evaluate the effects of CO₂-induced asphyxiation, dissection, and dissection time on brain oxylipin concentrations. Compared with head-focused microwave fixation (control), CO₂ followed by microwave fixation prior to dissection increased oxylipins derived from lipoxygenase (LOX), 15-hydroxyprostaglandin dehydrogenase (PGDH), cytochrome P450 (CYP), and soluble epoxide hydrolase (sEH) enzymatic pathways. This effect was enhanced when the duration of postmortem ischemia was prolonged by 6.4 min prior to microwave fixation. Brains dissected from rats subjected to CO₂ without microwave fixation showed greater increases in LOX, PGDH, CYP and sEH metabolites compared with all other groups, as well as increased cyclooxygenase metabolites. In nonmicrowave-irradiated brains, sEH metabolites and one CYP metabolite correlated positively and negatively with dissection time, respectively. This study presents new evidence that the dissection process and its duration increase brain oxylipin concentrations, and that this is preventable by microwave fixation. When microwave fixation is not available, lipidomic studies should account for dissection time to reduce these artifacts.—Hennebelle, M., A. H. Metherel, A. P. Kitson, Y. Otoki, J. Yang, K. S. S. Lee, B. D. Hammock, R. P. Bazinet, and A. Y. Taha. **Brain oxylipin concentrations following hypercapnia/ischemia: effects of brain dissection and dissection time.** *J. Lipid Res.* 2019. 60: 671–682.

Supplementary key words brain lipids • polyunsaturated fatty acid metabolites • lipid mediators

This study was supported by USDA National Institute of Food and Agriculture Hatch Project 1008787; the University of California, Davis Department of Food Science and Technology and College of Agriculture and Environmental Sciences (A.Y.T.); Natural Sciences and Engineering Research Council of Canada Grant 482597 (R.P.B.); National Institute of Environmental Health Sciences Grant R01 ES002710; and National Institute of Environmental Health Sciences Superfund Research Program Grant P42 ES004699 (B.D.H.); and National Institute of Environmental Health Sciences Grant R00 ES024806 (K.S.S.L.). The content is solely the responsibility of the authors and does not necessarily represent the official views of the National Institutes of Health. The authors declare no conflict of interest.

Manuscript received 8 February 2018 and in revised form 12 October 2018.

Published, *JLR Papers in Press*, November 21, 2018

DOI <https://doi.org/10.1194/jlr.D084228>

Copyright © 2019 Hennebelle et al. Published under exclusive license by The American Society for Biochemistry and Molecular Biology, Inc.

This article is available online at <http://www.jlr.org>

The brain is highly enriched in lipids, which make up approximately 60% of its dry weight (1, 2). Among them, PUFAs are important constituents of brain membrane phospholipids. The main PUFAs in the brain are n-6 arachidonic acid (ARA; 20:4n-6) and n-3 DHA (22:6n-3), which represent approximately 9% and 15% of total fatty acids, respectively (3, 4). Other less abundant PUFAs in the brain include n-6 linoleic acid (LNA; 18:2n-6), dihomo- γ -linolenic acid (20:3n-6), n-3 α -linolenic acid (ALA; 18:3n-3), and EPA (20:5n-3) (5). Irrespective of their abundance, these PUFAs, along with ARA and DHA, regulate several signaling processes within the brain (6–9).

PUFAs are precursors to oxidized metabolites, also known as oxylipins (10), that are synthesized by cyclooxygenase (COX) (11, 12), lipoxygenase (LOX) (13, 14), cytochrome P450 (CYP) (15–17), 15-hydroxyprostaglandin dehydrogenase (PGDH) (18, 19), and soluble epoxide hydrolase (sEH) enzymes (20, 21). In the brain, these enzymes synthesize hundreds of oxylipins from a limited number of PUFA precursors (22–26). Oxylipins regulate multiple physiological processes within the brain, including synaptic transmission (27–29), vasodilation (30, 31), angiogenesis (32), neuronal morphology (33, 34), blood flow (30), and pro- or anti-inflammatory signaling (35–40).

Abbreviations: ALA, α -linolenic acid; ARA, arachidonic acid; COX, cyclooxygenase; CYP, cytochrome P450; DGLA, dihomo- γ -linolenic acid; DiHDPE, dihydroxydocosapentaenoic acid; DiHETE, dihydroxyicosatetraenoic acid; DiHETrE, dihydroxyeicosatrienoic acid; DiHODE, dihydroxyoctadecadienoic acid; DiHOME, dihydroxyoctadecenoic acid; EpDPE, epoxydocosapentaenoic acid; EpETrE, epoxyeicosatrienoic acid; EpODE, epoxyoctadecadienoic acid; EpOME, epoxyoctadecenoic acid; ETE, eicosatetraenoic acid; HEPE, hydroxyeicosapentaenoic acid; HETrE, hydroxyeicosatrienoic acid; HOTrE, hydroxyoctadecatrienoic acid; LNA, linoleic acid; LOQ, limit of quantification; LOX, lipoxygenase; ODE, octadecadienoic acid; PG, prostaglandin; PGDH, 15-hydroxyprostaglandin dehydrogenase; sEH, soluble epoxide hydrolase; SPE, solid-phase extraction; TriHETrE, trihydroxyeicosatrienoic acid; TriHOME, trihydroxyoctadecenoic acid; TX, thromboxane; VIP, variable importance in the projection.

¹To whom correspondence should be addressed.

e-mail: ataha@ucdavis.edu

^SThe online version of this article (available at <http://www.jlr.org>) contains a supplement.

Ischemic brain injury stimulates the release of PUFAs esterified to brain membrane phospholipids (41, 42). While the majority of released PUFAs are reesterified into the membrane (43), a small portion is enzymatically converted into oxylipins that play a role in the brain's response to injury (35, 44). For instance, DHA-derived hydroxylated products and ARA-derived epoxidized metabolites produced following ischemic injury have been reported to exert neuroprotective effects by decreasing inflammation and apoptosis (44–46), inhibiting astrogliosis (36), activating mitochondria (46), promoting angiogenesis, and regulating blood flow (36, 38). Proinflammatory ARA-derived prostanoids and HETEs synthesized via the COX and LOX pathways have been shown to play an important role in the initial immune response following ischemic brain injury (47–50).

Understanding oxylipin metabolism and signaling in the brain is important due to their central role in regulating cerebral function and response to ischemia. The development of lipidomics (51) involving LC/MS/MS to characterize and quantify oxylipins (52, 53) has provided a new dimension to the brain field. Despite greatly improved analytical tools, one of the main challenges in studying brain oxylipin metabolism is to dissociate the effects of a specific treatment from artifacts generated during euthanasia that can induce postmortem changes in brain oxylipin concentrations (54–56).

Head-focused microwave fixation has been utilized as a method of euthanasia to prevent postmortem changes in brain lipid metabolism (41, 54, 56–58). Microwave fixation heat-denatures enzymes involved in lipid metabolism by applying a focused microwave beam to the top of the animal's head. The main advantage of this method is that it fixes brain metabolites in their current state, avoiding ischemia-related postmortem changes in oxylipins (55) and other important PUFA-derived mediators such as 2-arachidonoylglycerol (59) and *N*-arachidonylethanolamine (60).

Despite the advent of this technique in the 1970s (61–63), many laboratories continue to use standard CO₂ euthanasia protocols without microwave fixation to study brain lipid metabolism. CO₂ asphyxiation induces hypercapnia (i.e., elevated CO₂ in blood), resulting in increased blood flow, initially, to various tissues, including the brain (64). Prolonged hypercapnia leads to ischemia, the cessation of blood flow to the brain.

Although it is known that CO₂ euthanasia produces artifacts due to hypercapnia/ischemia, no study has investigated the potential impact of dissecting the brain and the time it takes to do so on exacerbating these changes. The dissection process itself involves penetrating the skull and periosteum layer to remove the brain and may represent a form of blunt-force trauma (65) that might induce changes in brain oxylipins. The duration of postmortem ischemia was previously shown to progressively increase brain unesterified PUFA concentrations (known as the Bazan effect) (42), and because unesterified PUFAs are precursors to oxylipins, it is possible that time-dependent changes in their postmortem concentrations correspond to changes in oxylipins.

This study tested the hypothesis that brain oxylipin concentrations will be affected by the dissection process and the duration of this process following CO₂-induced

hypercapnia/ischemia. Using a targeted lipidomics approach, we determined the effect of CO₂ asphyxiation with or without head-focused microwave fixation on 87 oxylipins (see supplemental Table S1 for a list of compounds and their abbreviations) and probed for correlations between dissection time and brain oxylipins. In view of a study showing that some enzymes maintain their activity in organic solvents used for oxylipin extraction (66), a secondary aim was to confirm that our extraction protocol involving overnight incubation of brain homogenates in methanol does not alter oxylipin concentrations.

METHODS

Animals

One-month-old Long Evans male rats were obtained from Charles River (Saint-Constant, Canada). The rats were housed two per cage and were fed a standard rat chow (2018 Teklad Global 18% protein rodent diet; Envigo, Madison, WI) containing 186 g/kg crude protein, 62 g/kg fat, 554 g/kg carbohydrates, 35 g/kg crude fiber, 53 g/kg ash, and 110 g/kg moisture for 30 days. The fatty acid composition of the diets, as previously analyzed, was 18.5% palmitic acid (16:0), 2.8% stearic acid (18:0), 18.5% oleic acid (18:1n-9), 54.8% LNA, and 5.6% ALA (67). All procedures were performed in accordance with the Canadian Council on Animal Care and were approved by the University of Toronto Animal Ethics Committee.

Following 30 days from the time of arrival, the rats were randomized into four groups as shown in **Fig. 1**. Rats in group 1 (control, no ischemia; $n = 8$) were euthanized by head-focused microwave fixation (13.5 kW for 1.6 s; Cober Electronics Inc., Norwalk, CT) and decapitated, and their brains were dissected. Rats in group 2 ($n = 7$) were subjected to CO₂ asphyxiation for 2 min followed by head-focused microwave fixation, decapitation, and dissection. Rats in group 3 ($n = 8$) were subjected to CO₂ asphyxiation for 2 min followed by decapitation and a 6.4 ± 2.4 min wait prior to head-focused microwave fixation of the decapitated head and subsequent brain dissection. The rationale for waiting 6.4 min prior to microwave fixation was to account for the 6.6 ± 2.5 min it took us to remove the brains from the rats in group 4 ($n = 8$), which were subjected to CO₂ asphyxiation for 2 min followed by decapitation and brain dissection. Hence, unlike those in groups 1–3, rats in group 4 were not subjected to high-energy microwave fixation. Prior to being euthanized, all rats were weighed and recorded (means \pm SDs) as follows: group 1, 332 ± 20 g; group 2, 313 ± 20 g; group 3, 318 ± 20 g; and group 4, 323 ± 26 g. There were no statistically significant differences between the groups by one-way ANOVA ($P > 0.05$). All excised brains were flash-frozen in liquid nitrogen and transferred to a -80°C freezer. Samples were shipped on dry ice from Toronto, Canada to Davis, CA, where they were stored at -80°C until further analysis.

Dissection time was recorded with a stopwatch. Time was recorded for all rats except for one in group 4, which was unintentionally missed.

Oxylipin extraction

Unesterified oxylipins were extracted from whole brain samples using solid-phase extraction (SPE) as previously described (52, 68). One brain hemisphere weighing approximately 800 mg was homogenized for 3 min with a bead homogenizer in 800 μl methanol extraction solvent containing 0.1% acetic acid, 0.1% butylated hydroxytoluene, 10 μl antioxidant solution containing

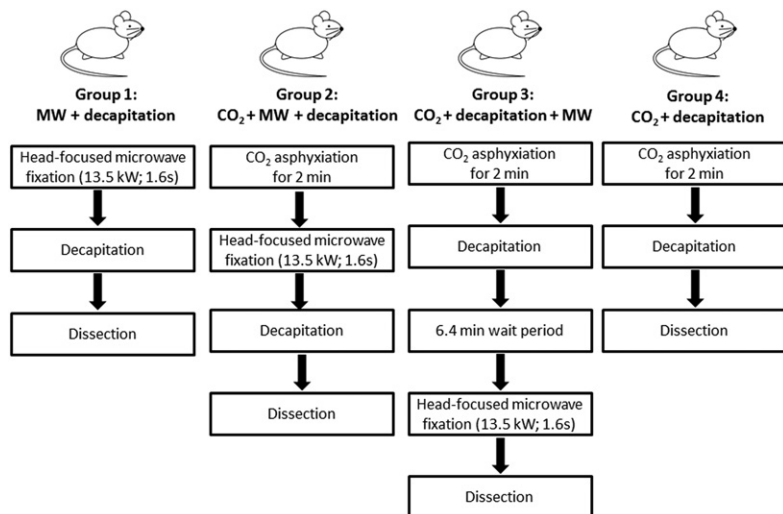


Fig. 1. Study design. Following 30 days of acclimatization, male Long Evans rats were randomly separated into 4 groups: group 1, MW + decapitation, in which rats were subjected to head-focused microwave fixation (13.5 kW for 1.6 s) prior to dissection (no ischemia; $n = 8$); group 2, CO₂ + MW + decapitation, in which rats were subjected to CO₂-induced asphyxiation for 2 min immediately followed by head-focused microwave fixation prior to dissection ($n = 7$); group 3, CO₂ + decapitation + MW, in which rats were subjected to CO₂-induced asphyxiation for 2 min, decapitated (and the decapitated heads left on the bench for an average of 6.38 min), and then subjected to microwave fixation prior to dissection ($n = 8$); and group 4, CO₂ + decapitation, in which rats were subjected to CO₂-induced asphyxiation for 2 min and then dissection ($n = 8$). The dissection time of group 3 (6.4 min) was matched to the dissection time of group 4 (6.6 min), which did not receive head-focused microwave irradiation. All brains were flash-frozen in liquid nitrogen after dissection. MW, microwave.

0.2 mg/ml butylated hydroxytoluene, EDTA and triphenylphosphine in water-methanol (1:1), and 20 μ l surrogate standard solution containing 500 nM $d_{11-11,12}$ -epoxyeicosatrienoic acid (EpETrE), $d_{11-14,15}$ -dihydroxyeicosatrienoic acid (DiHETrE), d_4 -6-keto-prostaglandin (PG) F_{1 α} , d_4 -9-HODE, d_4 -leukotriene B₄, d_4 -PGE₂, d_4 -thromboxane B₂ (TXB₂), d_6 -20-HETE, and d_8 -5-HETE in methanol. The homogenized samples were kept overnight at -80°C .

Samples were vortexed and centrifuged at 15,871 g for 10 min at 4°C the following day. Half of the supernatant was used for the extraction and was poured into a 60 mg Oasis HLB 3cc SPE column (Waters, Milford, MA) that was prerinsed with 1 vol ethyl acetate and 2 vol methanol and preconditioned with 2 vol SPE buffer containing 5% methanol and 0.1% acetic acid in ultrapure water (Millipore, Bedford, MA). The columns were then rinsed twice with SPE buffer before being subjected to 20 min of vacuum (~ 20 psi). Oxylipins were eluted with 0.5 ml methanol and 1.5 ml ethyl acetate in a 2 ml centrifuge tube containing 6 μ l 30% glycerol solution in methanol.

Samples were dried under nitrogen and dissolved in 50 μ l methanol containing 200 nM 1-cyclo-hexyl ureido, 3-dodecanoic acid and filtered by centrifugation at 15,871 g for 20 min at 4°C in Ultrafree-MC PVDF filters (0.1 μ m; Millipore). The recovery of the surrogate standard was determined by dividing the observed area of a known amount of deuterated standard added to the brain sample preextraction by the area of equimolar amounts of the same deuterated standard run on the LC/MS/MS without extraction. Mean standard percentage recoveries for all groups (combined and individually) are shown in supplemental Table S2. As shown, the percentage recovery of d_8 -5 HETE, $d_{11-11,12}$ -EpETrE, d_4 -leukotriene B₄, d_4 -6-keto-PGF_{1 α} , d_4 -PGE₂, d_4 -9-HODE, $d_{11-14,15}$ -DiHETrE, and d_4 -TXB₂ was 13, 16, 16, 25, 59, 16, 16, and 22%, respectively.

Effect of overnight storage of extracted samples

To confirm that overnight incubation in extraction solvent did not alter oxylipin concentrations, we used the remaining brain samples from a prior study in which the cortex, cerebellum, hippocampus, and brain stem from nonmicrowaved rats had been removed following CO₂ asphyxiation, decapitation, and dissection ($n = 3$). These remaining samples weighed approximately 500 mg and were homogenized in 400 μ l extraction solvent containing the surrogate standard and antioxidant mixture. The samples were centrifuged, and the supernatant containing oxylipins was split into two, one for direct extraction (200 μ l) and

the other for overnight incubation (with the brain homogenate) at -80°C prior to extraction (200 μ l). Each extract was subjected to SPE and LC/MS/MS analysis as described below.

LC/MS/MS

Eighty-seven oxylipins (supplemental Table S1) were analyzed by ultrahigh-pressure LC/MS/MS as previously described (52, 68) using an Agilent 1200SL (Agilent Technologies, Palo Alto, CA) ultrahigh-pressure LC system connected to a 4000 QTRAP tandem mass spectrometer (Applied Biosystems Instrument Corporation, Foster, CA) equipped with an electrospray ion source. A 2.1×150 mm ZORBAX Eclipse Plus C18 column with a 1.8 μ m particle size was used to separate oxylipins. Calibration curves for each of the 87 oxylipins analyzed were produced using Cayman Chemicals (Ann Arbor, MI) standards or synthetic standards made in Dr. Bruce Hammock's laboratory.

The autosampler and the column were kept at 4 and 50°C , respectively. The mobile phase A was 0.1% acetic acid in ultrapure water, and the mobile phase B was acetonitrile-methanol-acetic acid (84:16:0.1). The flow rate was maintained at 0.25 ml/min for a total run time of 21 min. Mobile phase B was held at 35% for 0.25 min and then increased to 45% from 0.25 to 1 min, to 55% from 1 to 3 min, to 65% from 3 to 8.5 min, to 72% from 8.5 to 12.5 min, to 82% from 12.5 to 15 min, and to 95% from 15 to 16.5 min. This was followed by a 1.5 min hold (at 95% of mobile phase B), which was decreased to 35% from 18 to 18.1 min and held for 2.9 min. The instrument was operated in negative ESI mode. Parent and product ions used to identify each oxylipin by multiple reaction monitoring are shown in supplemental Table S1. Peaks were quantified according to standard curves generated for each oxylipin and corrected for the surrogate standard recovery using Analyst software version 1.4.2 (Applied Biosystems Instrument Corporation).

Due to instrument availability at the time, oxylipins obtained from the brain samples extracted immediately after homogenization or after overnight incubation in extraction solvent were analyzed on a 1290 Infinity ultrahigh-pressure LC coupled to a 6460 QqQ MS/MS system equipped with an electrospray ion source (Agilent Technologies), using a method adapted from the one described above. Briefly, oxylipins were separated using a 2.1×150 mm ZORBAX Eclipse Plus C18 column with a 1.8 μ m particle size. The mobile phase A consisted of 0.1% acetic acid in ultrapure water; the mobile phase B of acetonitrile-methanol (80:15) contained 0.1% acetic acid. The gradient program started at 35% B, increased to 40% B from 0 to 3 min, increased to 48% B from 3 to

4 min, increased to 60% B from 4 to 10 min, increased to 70% B from 10 to 20 min, increased to 85% B from 20 to 24 min, held at 85% B from 24 to 24.5 min, increased to 99% B from 24.5 to 24.6 min, held at 99% from 24.6 min to 26 min, decreased to 35% B from 26 to 26.1 min, and held at 35% B until 28 min.

The flow rate was 0.3 ml/min from 0 to 3 min. It was reduced to 0.25 ml/min between 3 and 24.6 min, increased to 0.35 ml/min from 24.6 to 27.3 min, and then decreased to 0.3 ml/min until 28 min. The volume of injection was 10 μ l. In total, 72 metabolites (instead of 87) were quantified with this method because ALA-derived epoxides and ALA- and DHA-derived dihydroxy standards were not incorporated into the Agilent QqQ platform at the time.

The limit of quantification (LOQ) for both ultrahigh-pressure LC/MS/MS methods was set at three times the lowest detectable concentration used in the standard curve. Oxylipins with more than 30% missing values (below LOQ) in at least one group were not subjected to statistical analysis.

All samples were extracted and run on LC/MS/MS in a blinded and randomized manner. Sample identity and grouping were revealed prior to statistical analysis.

Sample size justification

The sample size of seven to eight rats per group was based on a previous experiment comparing brain oxylipin profiles of rats subjected to CO₂-induced ischemia to those euthanized with head-focused microwave fixation (29). This sample size was sufficient to detect significant effects of CO₂-induced ischemia on brain oxylipin concentrations at a significance level α of 0.05 and a statistical power (1 - β) of 0.8.

Statistical analysis

Data are expressed as means \pm SDs. Values below the limit of detection were imputed by dividing the lowest quantifiable concentration on the standard curve by the square root of 2 [LOQ/sqrt(2)]. Statistical analysis was performed on log-transformed data because the data were not normally distributed based on the Shapiro-Wilk normality test.

Multivariate statistical analysis was performed on the log-transformed data using MetaboAnalyst version 3.0 to explore distinct data clustering among the groups (69, 70). Data were mean-centered and scaled to SDs. Unsupervised principal component analysis was performed to identify possible outliers and trends. Partial least-squares discriminant analysis was then applied to look at differences in oxylipin profiles between the groups. The variable importance in the projection (VIP) was used to determine the contribution of each metabolite to the difference between the groups. A VIP value >1 was considered as a significant discriminant. Validation of the model was performed using R^2 and Q^2 values derived from a 10-fold cross-validation algorithm and 2,000 permutation tests.

A one-way ANOVA followed by Tukey's post hoc multiple comparison test was used to determine statistical differences in the log-transformed oxylipin concentration data among the four groups using GraphPad Prism version 6.05 (GraphPad Software, Inc., La Jolla, CA). Statistical significance was set at $P < 0.05$ (two-tailed).

Oxylipins showing a significant difference between groups with the one-way ANOVA analysis were represented on a heat map using Euclidean distance and Ward's clustering analysis in MetaboAnalyst version 3.0 (69, 70).

Spearman's correlation was performed on nontransformed data using GraphPad Prism version 6.05 to determine the correlation between oxylipin concentrations and dissection time in each of the four groups. It should be noted that the sample size for the

CO₂ + decapitation group (group 4) was seven instead of eight because the dissection time was missing from one rat. Statistical significance was set at $P < 0.05$ (two-tailed).

A paired *t*-test was used to compare log-transformed oxylipin concentrations between samples extracted directly after homogenization or kept overnight at -80°C . Statistical significance was set at $P < 0.05$ (one-tailed).

RESULTS

Duration of dissection

One-way ANOVA showed that the duration of brain dissection did not differ significantly between the groups. It took 5.3 ± 1.4 ($n = 8$), 4.7 ± 1.3 ($n = 7$), 6.4 ± 2.4 ($n = 8$), and 6.6 ± 2.5 ($n = 7$) min to dissect brains from groups 1–4, respectively.

Overall oxylipin profile

In total, 55 of the 87 measured oxylipins were detected and had values above the LOQ in more than 70% of samples in at least one group. This included 12, 2, 24, 4, 4, and 9 metabolites derived from LNA, dihomo- γ -linolenic acid (DGLA), ARA, ALA, EPA, and DHA, respectively (Table 1).

Multivariate analysis

Unsupervised principal component analysis revealed a separation of the samples according to their experimental group and the absence of any outliers (data not shown). To further explore these differences, a partial least-squares discriminant analysis was performed. This resulted in a three-component model with a goodness of prediction Q^2 of 0.76 and a goodness of fit R^2 of 0.93 (Fig. 2).

VIP analysis revealed that changes in epoxy, hydroxy, dihydroxy, and prostanoid oxylipins explained the differences between the groups. The most discriminant oxylipins (VIP >1.5) were ARA-derived 15-oxo-eicosatetraenoic acid (ETE), 14,15- and 11,12-DiHETrE, and 11,12- and 14,15-EpETrE and ALA-derived 15,16-dihydroxyoctadecadienoic acid (DiHODE). Other metabolites such as ARA-derived hydroxy compounds (8-, 5-, 9-, and 20-HETE), dihydroxy compounds [8,9-DiHETrE and 5,15-dihydroxyeicosatetraenoic acid (DiHETE)], and PGs (PGJ₂, PGD₁, PGD₂, 6-keto-PGF_{1 α}); DHA-derived epoxides [19,20-, 16,17-, and 13,14-epoxydocosapentaenoic acid (EpDPE)] and dihydroxy compounds [16,17- and 10,11-dihydroxydocosapentaenoic acid (DiHDPE)]; LNA-derived 12,13-dihydroxyoctadecenoic acid (DiHOME) and 9,12,13- and 9,10,13-trihydroxyoctadecenoic acid (TriHOME); ALA-derived 15,16-epoxyoctadecadienoic acid (EpODE); and EPA-derived 8-hydroxyeicosapentaenoic acid (HEPE) also presented an important contribution to the variance (VIP >1) explaining the differences between the four groups.

Brain oxylipin concentrations

Table 1 presents oxylipin concentrations in rats 1) decapitated directly after microwave fixation (group 1); 2) decapitated after 2 min of CO₂ asphyxiation followed by microwave fixation (group 2); 3) subjected to CO₂

TABLE 1. Brain oxylipin concentrations (pmol/g wet weight)

	Group 1: MW + Decapitation (n = 8)	Group 2: CO ₂ + MW + Decapitation (n = 7)	Group 3: CO ₂ + Decapitation + MW (n = 8)	Group 4: CO ₂ + Decapitation (n = 8)	ANOVA (P Value)
LNA-derived metabolites					
9-HODE	6.3 ± 1.9 ^a	5.6 ± 2.2 ^a	6.4 ± 2.6 ^a	9.4 ± 1.4 ^b	0.0059
13-HODE	7.3 ± 2.3 ^{a,b}	6.4 ± 1.9 ^a	7.5 ± 2.8 ^{a,b}	10.3 ± 2.0 ^b	0.025
9-oxo-ODE	5.8 ± 2.2	4.3 ± 1.6	6.7 ± 5.4	7.0 ± 3.1	NS
13-oxo-ODE	0.4 ± 0.2 ^a	0.5 ± 0.6 ^a	0.6 ± 0.5 ^{a,b}	1.3 ± 0.5 ^b	0.0198
12(13)-EpOME	4.0 ± 2.1	3.3 ± 0.7	3.8 ± 1.6	4.6 ± 2.3	NS
9(10)-EpOME	2.7 ± 1.0	2.6 ± 0.8	2.5 ± 0.7	3.8 ± 1.8	NS
12,13-DiHOME	1.7 ± 0.3 ^a	2.4 ± 0.5 ^b	2.7 ± 0.5 ^b	3.2 ± 0.9 ^b	0.0002
9,10-DiHOME	1.0 ± 0.3 ^a	1.0 ± 0.2 ^{a,b}	1.0 ± 0.2 ^a	1.5 ± 0.4 ^b	0.0127
9,12,13-TriHOME	1.6 ± 0.4 ^a	1.5 ± 0.8 ^a	1.3 ± 0.3 ^a	2.9 ± 0.4 ^b	<0.0001
9,10,13-TriHOME	0.3 ± 0.1 ^a	0.3 ± 0.2 ^a	0.3 ± 0.07 ^a	0.5 ± 0.09 ^b	0.002
THF diols	0.2 ± 0.08	0.1 ± 0.02	0.1 ± 0.02	0.1 ± 0.04	NS
EKODE	0.7 ± 0.2	0.6 ± 0.08	0.7 ± 0.1	0.7 ± 0.1	NS
DGLA-derived metabolites					
15(S)-HETrE	0.3 ± 0.2 ^a	0.5 ± 0.6 ^a	0.9 ± 1.4 ^a	4.3 ± 2.3 ^b	0.0001
PGD ₁	0.05 ± 0.01 ^a	0.08 ± 0.1 ^a	0.06 ± 0.02 ^a	1.2 ± 0.3 ^b	<0.0001
ARA-derived metabolites					
5-HETE	0.6 ± 0.1 ^a	1.7 ± 0.7 ^b	4.1 ± 3.3 ^{b,c}	5.3 ± 2.5 ^c	<0.0001
8-HETE	0.2 ± 0.04 ^a	0.5 ± 0.2 ^a	2.2 ± 1.7 ^b	3.7 ± 1.7 ^b	<0.0001
9-HETE	0.3 ± 0.2 ^a	0.3 ± 0.1 ^a	1.1 ± 0.8 ^b	1.4 ± 0.8 ^b	0.0003
11-HETE	1.2 ± 1.8 ^a	2.7 ± 4.5 ^{a,b}	6.3 ± 8.3 ^b	23.7 ± 8.7 ^c	<0.0001
12-HETE	0.7 ± 1.0 ^a	4.3 ± 6.0 ^a	17.2 ± 21.4 ^b	108.6 ± 70.7 ^c	<0.0001
15-HETE	3.4 ± 2.8 ^a	9.7 ± 11.0 ^a	17.9 ± 22.7 ^a	54.2 ± 24.2 ^b	<0.0001
20-HETE	2.0 ± 1.1 ^a	2.6 ± 1.6 ^{a,b}	5.3 ± 3.1 ^{b,c}	5.7 ± 2.3 ^c	0.0006
8,15-DiHETE	0.2 ± 0.1	0.1 ± 0.08	0.2 ± 0.08	0.3 ± 0.2	NS
5,15-DiHETE	0.04 ± 0.03 ^a	0.05 ± 0.03 ^a	0.03 ± 0.01 ^a	0.1 ± 0.06 ^b	<0.0001
5-oxo-EETE	4.3 ± 3.5	6.4 ± 5.3	10.9 ± 10.4	5.5 ± 3.7	NS
15-oxo-EETE	0.3 ± 0.3 ^a	2.1 ± 1.0 ^b	5.1 ± 3.2 ^b	2.3 ± 1.3 ^b	<0.0001
8(9)-EpETrE	0.02 ± 0.0 ^a	0.04 ± 0.02 ^a	0.1 ± 0.04 ^b	0.3 ± 0.1 ^c	<0.0001
11(12)-EpETrE	2.4 ± 1.3 ^a	34.8 ± 12.3 ^b	51.8 ± 17.4 ^{b,c}	94.1 ± 62.1 ^c	<0.0001
14(15)-EpETrE	2.2 ± 0.9 ^a	44.2 ± 18.4 ^b	62.3 ± 20.5 ^b	127.8 ± 81.6 ^c	<0.0001
8,9-DiHETrE	0.08 ± 0.03 ^a	0.1 ± 0.06 ^{a,b}	0.2 ± 0.1 ^b	0.2 ± 0.1 ^b	0.0002
11,12-DiHETrE	0.2 ± 0.06 ^a	0.2 ± 0.05 ^{a,b}	0.4 ± 0.1 ^c	0.4 ± 0.1 ^{b,c}	<0.0001
14,15-DiHETrE	0.1 ± 0.05 ^a	0.3 ± 0.09 ^b	0.7 ± 0.1 ^c	0.6 ± 0.2 ^c	<0.0001
11,12,15-TriHETrE	0.5 ± 0.8 ^a	0.7 ± 1.1 ^{a,b}	1.3 ± 1.3 ^{a,b}	1.9 ± 0.9 ^b	0.0095
6-keto-PGF _{1α}	0.2 ± 0.1 ^a	0.6 ± 1.2 ^a	0.3 ± 0.3 ^a	25.7 ± 12.5 ^b	<0.0001
PGF _{2α}	0.9 ± 1.1 ^a	1.5 ± 3.1 ^a	2.0 ± 1.8 ^a	13.2 ± 3.1 ^b	<0.0001
PGE ₂	0.4 ± 0.7 ^a	0.4 ± 0.9 ^a	0.6 ± 0.5 ^a	4.7 ± 1.3 ^b	<0.0001
PGD ₂	0.4 ± 0.4 ^a	1.8 ± 4.2 ^a	0.8 ± 1.5 ^a	52.3 ± 13.8 ^b	<0.0001
PGJ ₂	0.07 ± 0.03 ^a	0.1 ± 0.2 ^a	0.08 ± 0.04 ^a	1.7 ± 0.6 ^b	<0.0001
TXB ₂	0.2 ± 0.1 ^a	1.8 ± 4.6 ^a	0.8 ± 1.4 ^a	23.0 ± 9.8 ^b	<0.0001
ALA-derived metabolites					
9-HOTrE	0.1 ± 0.05	0.2 ± 0.05	0.2 ± 0.09	0.2 ± 0.09	NS
13-HOTrE	0.3 ± 0.1 ^a	0.3 ± 0.1 ^{a,b}	0.2 ± 0.07 ^a	0.5 ± 0.1 ^b	0.0064
15(16)-EpODE	0.7 ± 0.5	0.5 ± 0.2	0.3 ± 0.1	1.0 ± 0.9	NS
15,16-DiHODE	0.6 ± 0.2 ^a	0.9 ± 0.3 ^{a,b}	1.2 ± 0.3 ^b	1.0 ± 0.4 ^b	0.0017
EPA-derived metabolites					
8-HEPE	0.3 ± 0.4	1.5 ± 1.1	1.8 ± 2.6	1.1 ± 0.7	NS
17(18)-EpETE	0.2 ± 0.2	0.1 ± 0.08	0.2 ± 0.1	0.2 ± 0.2	NS
11(12)-EpETE	0.06 ± 0.1	0.04 ± 0.03	0.08 ± 0.1	0.2 ± 0.3	NS
17,18-DiHETE	0.6 ± 0.2	0.5 ± 0.09	0.6 ± 0.2	0.5 ± 0.1	NS
DHA-derived metabolites					
19(20)-EpDPE	1.7 ± 0.9 ^a	3.8 ± 1.4 ^b	6.9 ± 2.8 ^{b,c}	17.0 ± 15.9 ^c	<0.0001
16(17)-EpDPE	0.7 ± 0.6 ^a	1.6 ± 1.0 ^{a,b}	3.4 ± 1.7 ^{b,c}	9.8 ± 7.6 ^c	<0.0001
13(14)-EpDPE	0.8 ± 0.7 ^a	1.3 ± 0.7 ^{a,b}	3.0 ± 0.9 ^{b,c}	7.4 ± 6.6 ^c	<0.0001
10(11)-EpDPE	1.0 ± 0.9 ^a	1.6 ± 0.5 ^{a,b}	3.0 ± 1.4 ^{b,c}	7.7 ± 6.2 ^c	<0.0001
16,17-DiHDPE	0.1 ± 0.1 ^a	0.1 ± 0.08 ^{a,b}	0.3 ± 0.2 ^b	0.3 ± 0.2 ^b	0.0159
13,14-DiHDPE	0.1 ± 0.1	0.1 ± 0.05	0.1 ± 0.06	0.2 ± 0.07	NS
10,11-DiHDPE	0.06 ± 0.03 ^a	0.07 ± 0.02 ^a	0.1 ± 0.04 ^b	0.2 ± 0.06 ^b	<0.0001
4,5-DiHDPE	1.6 ± 1.0	1.4 ± 1.0	0.8 ± 0.4	1.2 ± 0.6	NS
17-HDoHE	2.3 ± 1.3 ^a	2.9 ± 2.2 ^a	2.6 ± 2.4 ^a	13.2 ± 7.7 ^b	0.0002

Data are means ± SDs. Data were analyzed using a one-way ANOVA on log-transformed data followed by Tukey's multiple comparison test. Different superscript letters identify significant differences between groups for each metabolite. EKODE, epoxyketo-octadecenoic acid; EpETE, epoxyeicosatetraenoic acid; HDoHE, hydroxydocosahexaenoic acid; MW, microwave; THF, tetrahydrofuran.

asphyxiation, decapitation, and then microwave fixation of the decapitated head 6.4 min later (group 3); and 4) decapitated after CO₂ asphyxiation without microwave fixation (group 4). To simplify the results and interpretation

of the data, our results focus primarily on comparing groups 2–4, respectively, to control group 1.

Microwave fixation following 2 min of CO₂ (group 2) resulted in significant changes in seven LNA, ARA, and

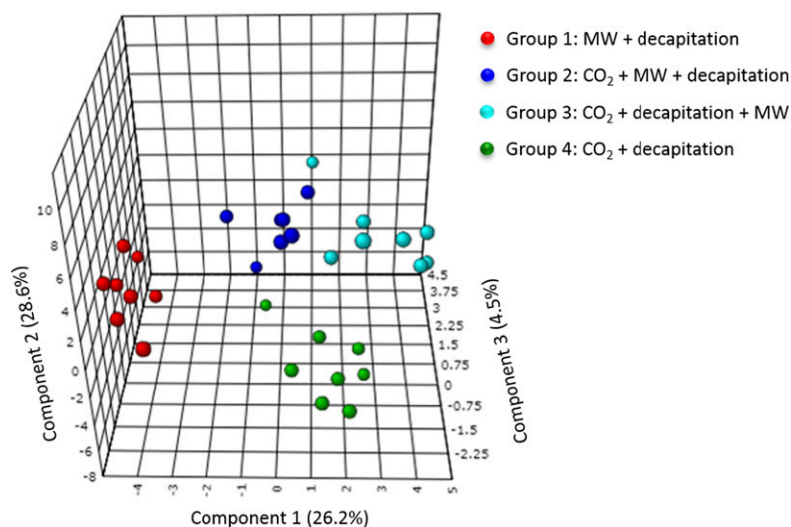


Fig. 2. Partial least-squares discriminant analyses comparing oxylin concentrations between the different experimental groups. The analysis resulted in a three-component model ($Q^2 = 0.76$; $R^2 = 0.93$). The MW + decapitation control group is represented in red (group 1), the CO₂ + MW + decapitation group is represented in dark blue (group 2), the CO₂ + decapitation + MW group is represented in light blue (group 3), and the CO₂ + decapitation group is represented in green (group 4). MW, microwave.

DHA metabolites compared with control rats killed with microwave fixation (no CO₂). LNA-derived 12,13-DiHOME, ARA-derived 5-HETE, 14,15-EpETrE, 11,12-EpETrE, 14,15-diHETrE and 15-oxo-ETE and DHA-derived 19,20-EpDPE were significantly increased by 1.4- to 20-fold in group 2 relative to group 1. Changes in hydroxy and ketone metabolites suggest the activation of LOX and PGDH pathways, respectively, whereas epoxy and dihydroxy changes reflect the activation of CYP and sEH pathways, respectively, following CO₂-induced hypercapnia/ischemia.

Microwave fixation following a 6.4 min wait after 2 min of CO₂-induced asphyxiation and decapitation (group 3) significantly increased the same 7 metabolites that were increased in group 2, as well as 14 additional ARA-, ALA-, and DHA-derived metabolites from the LOX, CYP, and sEH pathways, relative to group 1. The additional metabolites were ARA-derived 8-HETE, 9-HETE, 11-HETE, 12-HETE, 20-HETE, 8(9)-EpETrE, 8,9-DiHETrE, and 11,12-DiHETrE; ALA-derived 15,16-DiHODE; and DHA-derived 16,17-EpDPE, 13,14-EpDPE, 10,11-EpDPE, and their dihydroxy metabolites 16,17-DiHDPE and 10,11-DiHDPE. The 21 metabolites that changed in group 3 differed significantly from group 1. Specifically, ARA metabolites increased by 3- to 28-fold, the one ALA metabolite increased by 2-fold, and DHA metabolites increased by 1.7- to 4.9-fold. No significant differences were detected between groups 2 and 3 in the seven metabolites that increased relative to group 1.

Group 4 rats, which were subjected to 2 min of CO₂ and decapitated without microwave fixation, showed an increase in 40 metabolites, which differed significantly from group 1 and, in some cases, groups 2 and 3. Compared with microwave-irradiated controls (group 1), group 4 rats showed a 1.4- to 3-fold increase in LNA-derived 9- and 13-HODE, 13-oxo-octadecadienoic acid (ODE), 12,13-DiHOME, 9,12,13-TriHOME, and 9,10,13-TriHOME; a 14- and 24-fold increase in DGLA-derived 15(*S*)-hydroxyicosatrienoic acid (HETrE) and PGD₂; and a 1.7-fold increase in both ALA-derived 13-hydroxyoctadecatrienoic acid (HOTrE) and 15,16-DiHODE. Almost all detected ARA and DHA metabolites increased in group 4 compared with group 1. ARA-derived hydroxy compounds (HETEs) increased by

3- to 155-fold, epoxy metabolites (11,12- and 14,15-EpETrE) increased by 39- and 58-fold, dihydroxy (DiHETEs and DiHETrEs) and trihydroxy [11,12,15-trihydroxyicosatrienoic acid (TriHETrE)] metabolites increased by 2.5- to 6-fold, and COX-derived prostanoids and TXB₂ increased by 12- to 131-fold. Of the two detected epoxy ketones, 15-oxo-ETE increased by 7.7-fold. DHA-derived hydroxy, epoxy, and dihydroxy compounds increased by 3- to 14-fold in group 4 compared with group 1.

All metabolites that increased in groups 2 and 3 relative to controls were also statistically increased in group 4 compared with group 1, although the magnitude of change compared with group 1 was much greater in group 4. In many cases, group 4 LNA, ARA, and DHA metabolites differed significantly from groups 2 or 3 (Table 1).

Heat map and cluster analysis

Hierarchical cluster analysis using Ward's algorithm showed that metabolites within the CO₂ + decapitation group (group 4) clustered together and presented higher concentrations than the other groups (horizontal axis of Fig. 3), consistent with the one-way ANOVA findings (Table 1). Group 1 metabolites clustered together and showed the lowest concentration relative to the other three groups. Groups 2 and 3 tended to cluster together at intermediate concentrations between groups 1 and 4.

With regard to metabolite clustering (vertical axis of Fig. 3), CYP-derived epoxy metabolites and their respective diols derived from the sEH pathway tended to cluster together (vertical axis of Fig. 3), reflecting possible functional coupling of CYP and sEH enzymes.

Correlation between brain oxylin concentrations and dissection time

A correlation analysis was performed between all 55 detected brain metabolites and the time of dissection in each group to determine whether postmortem dissection time influences brain oxylin concentrations.

There was a significant correlation between 13,14-DiHDPE concentration and dissection time in group 1 ($r = -0.7857$; $P = 0.0279$; data not shown). No other significant associations between oxylin concentrations and dissection

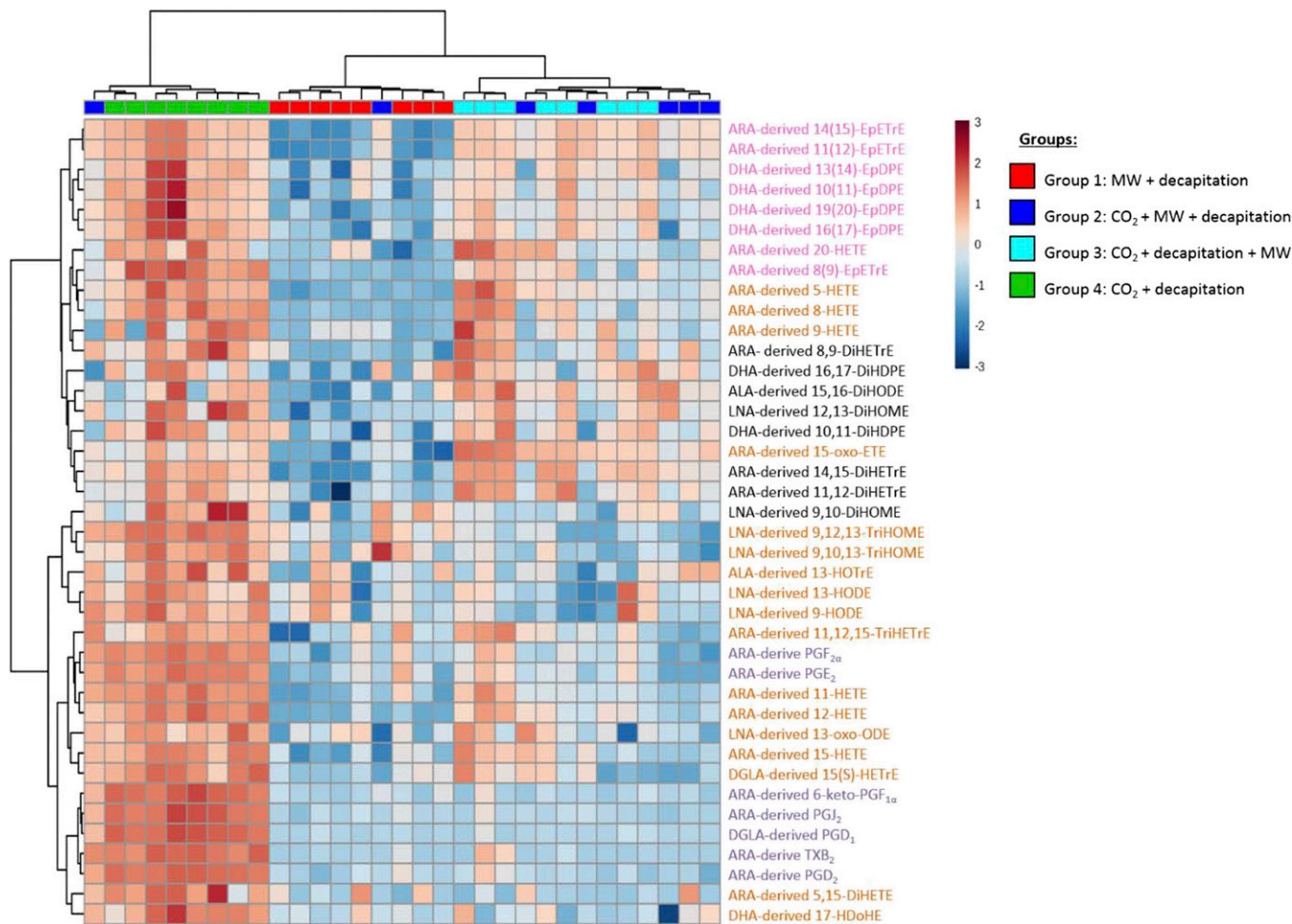


Fig. 3. Heat map representing metabolites that differed significantly among the groups based on one-way ANOVA. The color scale from -3 to 3 represents the z -score, which was calculated by dividing the difference between the metabolite concentration value and the metabolite group mean by the overall SD. A positive z -score reflects increased metabolite concentrations (i.e., increased red color intensity); a negative z -score reflects decreased metabolite concentrations (i.e., decreased blue color intensity). The colors on top of the heat map are the color codes for each group (group 1, red; group 2, dark blue; group 3, light blue; and group 4, green). Their position shows how the groups cluster together, as determined by hierarchical clustering using Ward's algorithm. Group 4 had the highest oxylipin concentrations, whereas group 1 had the lowest concentrations. Group 2 and group 3 clustered together with intermediate oxylipin concentrations. On the right side of the heat map are the metabolites themselves and their precursor fatty acid (e.g., ARA-derived 11-HETE). Metabolites in purple are derived from the COX pathway, those in orange are derived from the LOX pathway, those in pink are derived from the CYP pathway, and those in black are derived from the sEH pathway. The clustering of the PUFA-derived metabolites is depicted on the left side of the heat map. MW, microwave.

time were observed in groups 1 and 2, which were both subjected to microwave fixation prior to decapitation. In group 3, ARA-derived 8,9-EpETrE concentration was positively correlated to the time the brains were left decapitated on the bench prior to dissection ($r = 0.7381$; $P = 0.0458$; data not shown). No other significant correlations were detected in this group.

In group 4, which did not receive microwave irradiation following 2 min of CO₂ + decapitation, the duration of dissection was positively correlated to the ARA-derived dihydroxy metabolites 14,15-DiHETrE ($r = 0.9286$; $P = 0.0067$), 11,12-DiHETrE ($r = 0.8571$; $P = 0.0238$), 8,9-DiHETrE ($r = 0.8571$; $P = 0.0238$), and 8,15-DiHETE ($r = 0.8929$; $P = 0.0123$), as well as LNA-derived 12,13-DiHOME ($r = 0.8571$; $P = 0.0238$) and 9,10-DiHOME ($r = 0.7857$; $P = 0.048$) (Fig. 4). Dissection time was also inversely correlated to the concentration of EPA-derived 8-HEPE ($r = -0.929$; $P = 0.0067$) in this group (Fig. 4).

Overnight incubation in extraction solvent did not affect oxylipin concentrations in nonmicrowaved brains

To confirm that the overnight incubation of brain homogenates in extraction solvent did not alter oxylipin concentrations, we compared oxylipin concentrations in nonmicrowaved "rest-of-brain" homogenates (see Methods) kept overnight at -80°C prior to extraction or extracted directly after homogenization (from the same brain sample; $n = 3$). As shown in Fig. 5, no significant changes in oxylipin concentrations were observed between the two extraction protocols.

Summary of findings

Compared with microwave-irradiated controls, CO₂-induced hypercapnia/ischemia (2 min) followed by microwave fixation increased the concentration of nine oxylipins linked to the LOX, CYP, sEH, and PGDH pathways (group 2). This effect was enhanced when the duration of ischemia

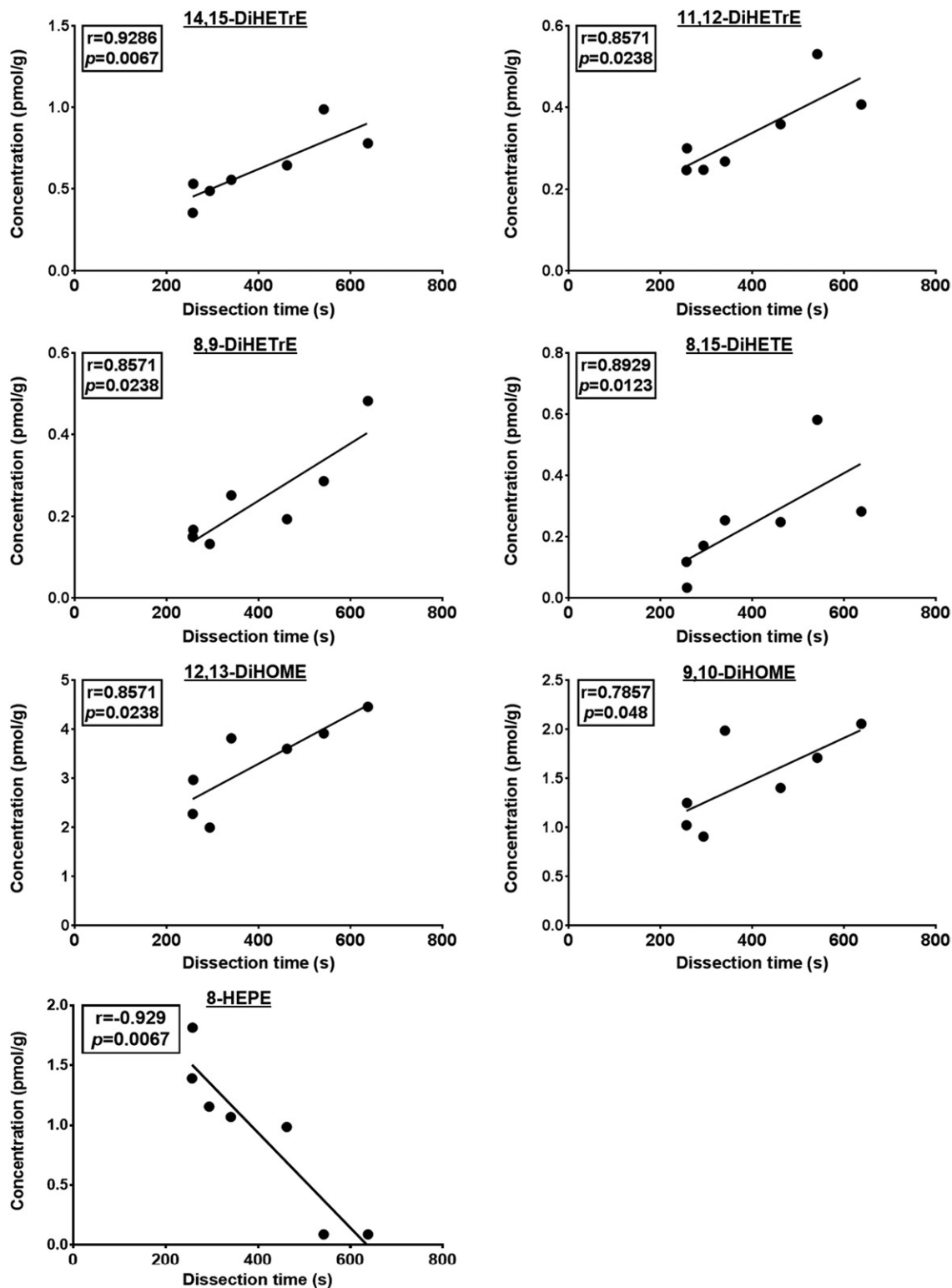


Fig. 4. Significant Spearman's correlation between oxylipin concentrations and dissection time in the CO₂ + decapitation group (group 4; n = 7). As outlined in Methods, the sample size was seven instead of eight because the duration of dissection was not collected for one rat.

was prolonged by decapitating the brain and applying microwave irradiation approximately 6 min later (group 3), as evidenced by the increase in 14 additional oxylipins (total of 21 oxylipins that changed). Brains dissected following CO₂-induced hypercapnia/ischemia without microwave fixation (group 4) showed significant increases in 40

oxylipins compared with group 1, including COX-derived prostanoids and TXB₂. In group 4, 20 of these metabolites also differed significantly from groups 2 and 3. The dissection time in group 4 was positively correlated to changes in sEH-derived diols and negatively to one epoxy EPA metabolite from CYP. Incubating nonmicrowave-irradiated brain

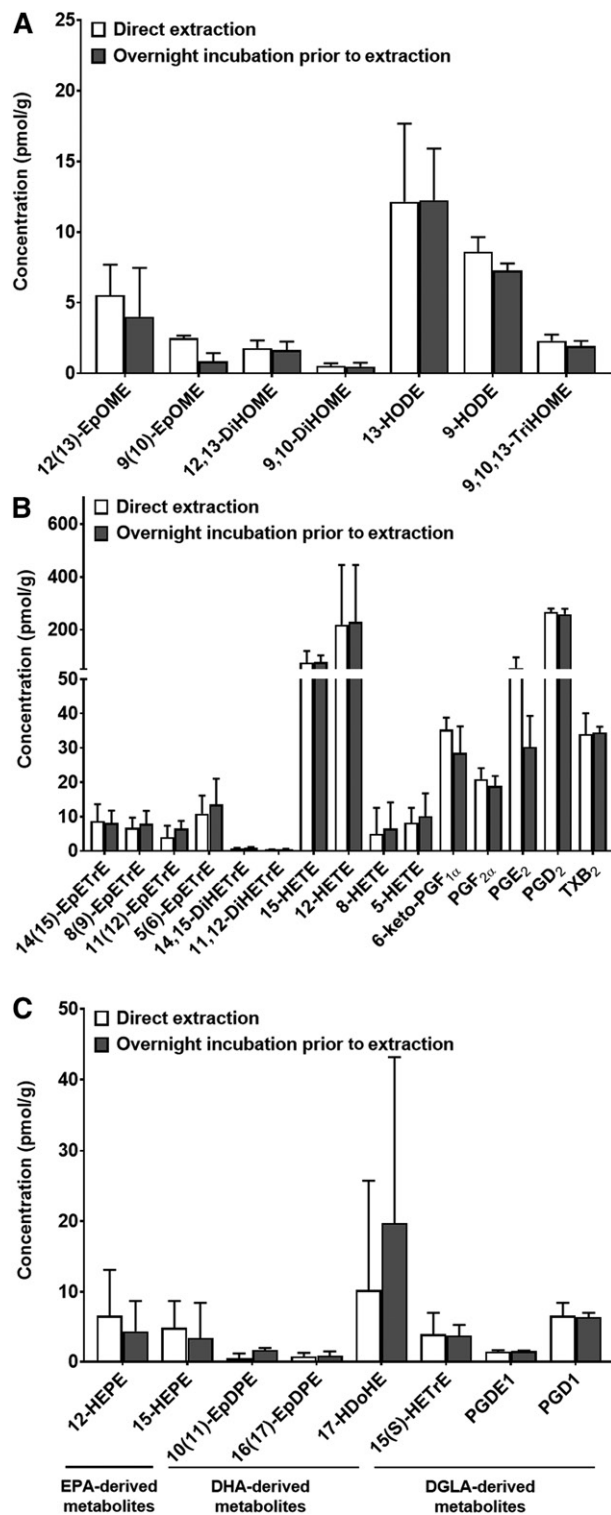


Fig. 5. Brains (500 mg) obtained from nonmicrowave-irradiated rats were homogenized in 400 μ l extraction solvent containing antioxidants and surrogate standard. The brain samples used were remaining parts following the removal of the cortex, cerebellum, hippocampus, and brainstem for oxylipin analysis in a separate study (29). Homogenized samples were split into two: one sample was extracted directly, while the other was kept overnight at -80°C (with the brain homogenate) prior to extraction. Oxylipins derived from (A) LNA, (B) ARA, and (C) EPA, DHA, and DGLA were detected and quantified. Log-transformed data were analyzed by a paired *t*-test. Data are means \pm SDs. There were no significant differences between the means ($P > 0.05$).

homogenates in methanol overnight at -80°C did not alter oxylipins compared with brains extracted immediately after homogenization.

DISCUSSION

This study shows that the time for brain removal is important and that variable time results in variable oxylipin concentrations. Compared with microwave-irradiated controls, CO_2 -induced hypercapnia/ischemia increased brain concentrations of PUFA-derived oxylipins linked to the LOX, CYP, sEH, and PGDH pathways in rats dissected after microwave fixation (group 2). This effect was enhanced when ischemia was sustained by decapitation (group 3). Dissecting brains from rats subjected to hypercapnia/ischemia without microwave fixation resulted in the greatest increase in oxylipins synthesized by LOX, CYP, sEH, and PGDH enzymes, as well as increased COX metabolites (group 4). In these nonmicrowave-fixated rats, dissection time correlated with several oxylipins.

Unlike a previous study (71), we did not observe a significant increase in COX metabolites in rats subjected to microwave irradiation after 2 min of CO_2 (group 2) compared with control rats, which received microwave irradiation but not CO_2 (group 1). This could be due to differences in the duration of CO_2 asphyxiation. Trepanier et al. (71) applied 5 min of CO_2 prior to microwave fixation and decapitation, whereas our rats were subjected to 2 min of CO_2 prior to microwave fixation and decapitation.

COX metabolites did not change in group 3 either, although the decapitated heads were left on the bench for 6.4 min at room temperature prior to microwave fixation. Farias et al. (54) reported an increase in brain COX metabolite concentrations when the decapitated head was maintained at 37°C for 5 min, suggesting a likely effect of temperature and the duration of decapitation [as Trepanier et al. (71) reported] on brain COX metabolite concentrations.

In group 3, the magnitude of changes in LOX, CYP, and sEH oxylipins, specifically ARA-derived epoxy (EpETrE), hydroxy (HETE), and dihydroxy (DiHETrE) metabolites, DHA-derived epoxy (EpDPE) and dihydroxy (DiHDPE) metabolites, LNA-derived 12,13-DiHOME metabolites, and ALA-derived 15,16-DiHODE metabolites, was much higher compared with groups 1 and 2. This suggests an independent effect of prolonged hypercapnia/ischemia caused by decapitation on LOX-, CYP-, and sEH-derived oxylipins, because the rats in group 3 were subjected to microwave fixation after CO_2 asphyxiation and leaving the decapitated heads on the bench for 6.4 min.

The marked increase in LOX, CYP, sEH, PGDH, and COX metabolites in group 4 compared with others could be attributed to the dissection process of physically removing the brains from the cranium. The dissection of the brain may be similar to blunt-force trauma. Although limited evidence is available to support this assertion (72), the mechanical penetration of the skull and periosteum layer encapsulating the brain is known to provoke a trauma-like event (65) that could induce oxylipin metabolic enzymes.

In humans, LOX-derived HETEs and thromboxane-derived metabolites were increased or detected in the cerebrospinal fluid of trauma patients compared with controls (73).

It is also possible that these changes are due to a cryogenic effect of flash-freezing the dissected and nonmicrowave-fixed brains (group 4) in liquid nitrogen. Flash-freezing decapitated brains or entire rats in liquid nitrogen has been shown to increase cyclic AMP, ATP, lactic acid, and other metabolites involved in brain energy metabolism compared with microwave-irradiated rats (61, 62, 74). Consistent with these observations, Golovko and Murphy (55) showed a significant increase in COX-derived prostanoids after flash-freezing dissected brains in liquid nitrogen compared with microwave irradiation. Trepanier et al. (71) also showed a significant increase in COX metabolites after subjecting rats to 5 min of CO₂ ischemia and placing the decapitated brains on dry ice for an additional 5 min prior to dissection. Golovko and Murphy (58) also reported increases in COX metabolites within 30 s of CO₂-induced brain ischemia and freezing the brains in liquid nitrogen, compared to microwave-irradiated controls. The mechanism linking rapid cooling to brain oxylipin metabolism is not understood, but similar to the dissection process, it likely involves multiple metabolic cascades, including the activation of receptor-mediated PUFA turnover pathways (75). This needs to be investigated in future studies.

Dissection time was positively correlated with LNA- and ARA-derived dihydroxy products of sEH (14,15-DiHETrE, 11,12-DiHETrE, 8,9-DiHETrE, 8,15-DiHETE, 12,13-DiHOME, and 9,10-DiHOME) and inversely with one EPA-derived epoxy metabolite of CYP (8-HEPE) in the CO₂ + decapitation group only (group 4). This correlation suggests that the duration of dissection specifically and proportionally alters LNA-, ARA-, and EPA-derived oxylipins synthesized by CYP and sEH enzymes in nonmicrowave-irradiated brains. This could add to the variability in studies that do not use microwave fixation, which is why it may be worthwhile to control for dissection time when a high-energy microwave is not available.

Some oxylipin extraction protocols, including ours, involve overnight incubation of homogenized samples in organic solvent at -80°C because this is thought to optimize oxylipin extraction from tissues (29, 68). Prolonged incubation in an extraction mixture containing acetone-saline (2:1; v:v) at room temperature has been reported to increase the concentration of PGs and TXB₂ in nonmicrowaved brains, suggesting that COX or other lipid metabolic enzymes might be active in extraction solvents such as acetone (55). In the present study, oxylipins were extracted in methanol solvent (containing 0.1% acetic acid, deuterated surrogate standard, and antioxidants) for 24 h at -80°C . To ensure that prolonged incubation in methanol did not produce artifacts, particularly in group 4, we performed the SPE immediately or 24 h after homogenizing the brain samples in methanol containing acetic acid, antioxidant mix, and deuterated surrogate standards (see Methods). No changes in oxylipin concentrations were observed following overnight incubation in extraction solvent (at -80°C) compared with immediate extraction, suggesting that

enzymes were not activated by prolonged incubation in the methanol containing acetic acid and antioxidant mix. Our findings also indicate that overnight incubation in solvent does not necessarily optimize oxylipin extraction as previously thought.


A limitation of this study is that the potential contribution of blood oxylipins to measured brain values was not studied. Blood accounts for approximately 2% of brain volume, which means that changes in brain oxylipins due to hypercapnia/ischemia dissection and/or freezing in liquid nitrogen could be attributed in part to oxylipin changes in blood vessels supplying the brain. Another limitation is the low percentage recovery (13–59%) of the surrogate quantitation standards used to control for losses in brain oxylipin extraction (supplemental Table S2, second column depicting mean percent recovery in “All Samples”). This could partly explain the high within-group variability (Table 1).

A low and comparable percentage recovery has been reported for deuterated surrogate standards extracted from brain and other tissues, likely due to losses during the SPE step (76). Although better methods are needed to improve oxylipin recovery from tissue matrices, losses in oxylipins in the SPE step are likely proportionally reflected in the surrogate. However, increasing surrogate standard and metabolite recovery might improve the precision associated with oxylipin quantitation and reduce the variability. Notably, the variability in the data are also due to the experimental design. It was higher, for instance, in the CO₂ + decapitation group compared with the microwave group, as expected.

Previous studies have attributed the effects of hypercapnia/ischemia to some ARA- and DHA-derived metabolites (54, 71). This study shows that several PUFA metabolites, including those derived from LNA, DGLA, and ALA, are also involved in the response to hypercapnia/ischemia and dissection. This is consistent with our recent study showing increased oxylipins derived from multiple PUFA precursors in various brain regions following hypercapnia/ischemia/dissection (29). Collectively, these findings suggest that LNA, DGLA, and ALA are involved in the response to ischemia-related brain injury similar to ARA and DHA, despite accounting for less than 2% of brain total fatty acids.

EPA metabolites did not differ significantly between the groups, likely because they were measured in whole brain rather than specific brain regions. In our previous study, EPA metabolites changed in the hippocampus and brainstem but not in the cortex and cerebellum following hypercapnia/ischemia, suggesting regional specificity of changes in EPA-derived oxylipins (29).

In summary, this study showed that hypercapnia/ischemia increases brain oxylipin concentrations and that this effect is further enhanced when the head is decapitated and when the brain is dissected and flash-frozen in liquid nitrogen. Dissection time also correlated with changes in several brain oxylipins, whereas overnight incubation in methanol extraction solvent had minimal effects. While our findings reaffirm the importance of using microwave irradiation to prevent artifacts linked to these postmortem processes (54, 55, 57, 71), it also identifies decapitation, dissection, dissection time, and potentially flash-freezing as

important factors that affect brain oxylipin concentrations independent of hypercapnia and postmortem ischemia. In studies that do not use microwave fixation, these confounders may introduce artifacts that must be considered when interpreting between-group differences or lack thereof. Microwave fixation overcomes these challenges. 

REFERENCES

- Johnson, A. C., A. R. McNabb, and R. J. Rossiter. 1949. Concentration of lipids in the brain of infants and adults. *Biochem. J.* **44**: 494–498.
- O'Brien, J. S., and E. L. Sampson. 1965. Lipid composition of the normal human brain: gray matter, white matter, and myelin. *J. Lipid Res.* **6**: 537–544.
- Fraser, T., H. Tayler, and S. Love. 2010. Fatty acid composition of frontal, temporal and parietal neocortex in the normal human brain and in Alzheimer's disease. *Neurochem. Res.* **35**: 503–513.
- McNamara, R. K., and S. E. Carlson. 2006. Role of omega-3 fatty acids in brain development and function: potential implications for the pathogenesis and prevention of psychopathology. *Prostaglandins Leukot. Essent. Fatty Acids.* **75**: 329–349.
- Taha, A. Y., M. Basselin, E. Ramadan, H. R. Modi, S. I. Rapoport, and Y. Cheon. 2012. Altered lipid concentrations of liver, heart and plasma but not brain in HIV-1 transgenic rats. *Prostaglandins Leukot. Essent. Fatty Acids.* **87**: 91–101.
- Bazinet, R. P., and S. Laye. 2014. Polyunsaturated fatty acids and their metabolites in brain function and disease. *Nat. Rev. Neurosci.* **15**: 771–785.
- Denis, I., B. Potier, C. Heberden, and S. Vancassel. 2015. Omega-3 polyunsaturated fatty acids and brain aging. *Curr. Opin. Clin. Nutr. Metab. Care.* **18**: 139–146.
- Karr, J. E., J. E. Alexander, and R. G. Winningham. 2011. Omega-3 polyunsaturated fatty acids and cognition throughout the lifespan: a review. *Nutr. Neurosci.* **14**: 216–225.
- Trépanier, M. O., K. E. Hopperton, S. K. Orr, and R. P. Bazinet. 2016. N-3 polyunsaturated fatty acids in animal models with neuroinflammation: an update. *Eur. J. Pharmacol.* **785**: 187–206.
- Gabbs, M., S. Leng, J. G. Devassy, M. Monirujjaman, and H. M. Aukema. 2015. Advances in our understanding of oxylipins derived from dietary PUFAs. *Adv. Nutr.* **6**: 513–540.
- Laneville, O., D. K. Breuer, N. Xu, Z. H. Huang, D. A. Gage, J. T. Watson, M. Lagarde, D. L. DeWitt, and W. L. Smith. 1995. Fatty acid substrate specificities of human prostaglandin-endoperoxide H synthase-1 and -2. Formation of 12-hydroxy-(9Z, 13E/Z, 15Z)-octadecatrienoic acids from alpha-linolenic acid. *J. Biol. Chem.* **270**: 19330–19336.
- Funk, C. D. 2001. Prostaglandins and leukotrienes: advances in eicosanoid biology. *Science.* **294**: 1871–1875.
- Chang, J., L. Jiang, Y. Wang, B. Yao, S. Yang, B. Zhang, and M. Z. Zhang. 2015. 12/15 Lipoxygenase regulation of colorectal tumorigenesis is determined by the relative tumor levels of its metabolite 12-HETE and 13-HODE in animal models. *Oncotarget.* **6**: 2879–2888.
- Murphy, E., W. Glasgow, T. Fralix, and C. Steenbergen. 1995. Role of lipoxygenase metabolites in ischemic preconditioning. *Circ. Res.* **76**: 457–467.
- Fer, M., L. Corcos, Y. Dreano, E. Plee-Gautier, J. P. Salaun, F. Berthou, and Y. Amet. 2008. Cytochromes P450 from family 4 are the main omega hydroxylating enzymes in humans: CYP4F3B is the prominent player in PUFA metabolism. *J. Lipid Res.* **49**: 2379–2389.
- Fer, M., Y. Dreano, D. Lucas, L. Corcos, J. P. Salaun, F. Berthou, and Y. Amet. 2008. Metabolism of eicosapentaenoic and docosahexaenoic acids by recombinant human cytochromes P450. *Arch. Biochem. Biophys.* **471**: 116–125.
- Arnold, C., M. Markovic, K. Blossy, G. Wallukat, R. Fischer, R. Dechend, A. Konkel, C. von Schacky, F. C. Luft, D. N. Muller, et al. 2010. Arachidonic acid-metabolizing cytochrome P450 enzymes are targets of [omega]-3 fatty acids. *J. Biol. Chem.* **285**: 32720–32733.
- Wendell, S. G., F. Golin-Bisello, S. Wenzel, R. W. Sobol, F. Holguin, and B. A. Freeman. 2015. 15-Hydroxyprostaglandin dehydrogenase generation of electrophilic lipid signaling mediators from hydroxy omega-3 fatty acids. *J. Biol. Chem.* **290**: 5868–5880.
- Snyder, N. W., F. Golin-Bisello, Y. Gao, I. A. Blair, B. A. Freeman, and S. G. Wendell. 2015. 15-Oxoeicosatetraenoic acid is a 15-hydroxyprostaglandin dehydrogenase-derived electrophilic mediator of inflammatory signaling pathways. *Chem. Biol. Interact.* **234**: 144–153.
- Greene, J. F., J. W. Newman, K. C. Williamson, and B. D. Hammock. 2000. Toxicity of epoxy fatty acids and related compounds to cells expressing human soluble epoxide hydrolase. *Chem. Res. Toxicol.* **13**: 217–226.
- Inceoglu, B., K. R. Schmelzer, C. Morisseau, S. L. Jinks, and B. D. Hammock. 2007. Soluble epoxide hydrolase inhibition reveals novel biological functions of epoxyeicosatrienoic acids (EETs). *Prostaglandins Other Lipid Mediat.* **82**: 42–49.
- Breder, C. D., D. Dewitt, and R. P. Kraig. 1995. Characterization of inducible cyclooxygenase in rat brain. *J. Comp. Neurol.* **355**: 296–315.
- van Leyen, K., H. Y. Kim, S. R. Lee, G. Jin, K. Arai, and E. H. Lo. 2006. Baicalein and 12/15-lipoxygenase in the ischemic brain. *Stroke.* **37**: 3014–3018.
- Chinnici, C. M., Y. Yao, and D. Pratico. 2007. The 5-lipoxygenase enzymatic pathway in the mouse brain: young versus old. *Neurobiol. Aging.* **28**: 1457–1462.
- Sarkar, P., J. Narayanan, and D. R. Harder. 2011. Differential effect of amyloid beta on the cytochrome P450 epoxygenase activity in rat brain. *Neuroscience.* **194**: 241–249.
- Sura, P., R. Sura, A. E. Enayetallah, and D. F. Grant. 2008. Distribution and expression of soluble epoxide hydrolase in human brain. *J. Histochem. Cytochem.* **56**: 551–559.
- Chen, C., and N. G. Bazan. 2005. Endogenous PGE2 regulates membrane excitability and synaptic transmission in hippocampal CA1 pyramidal neurons. *J. Neurophysiol.* **93**: 929–941.
- Sang, N., J. Zhang, V. Marcheselli, N. G. Bazan, and C. Chen. 2005. Postsynaptically synthesized prostaglandin E2 (PGE2) modulates hippocampal synaptic transmission via a presynaptic PGE2 EP2 receptor. *J. Neurosci.* **25**: 9858–9870.
- Hennebelle, M., Z. Zhang, A. H. Metherel, A. P. Kitson, Y. Otoki, C. E. Richardson, J. Yang, K. S. S. Lee, B. D. Hammock, L. Zhang, et al. 2017. Linoleic acid participates in the response to ischemic brain injury through oxidized metabolites that regulate neurotransmission. *Sci. Rep.* **7**: 4342.
- Ellis, E. F., R. J. Police, L. Yancey, J. S. McKinney, and S. C. Amruthesh. 1990. Dilation of cerebral arterioles by cytochrome P-450 metabolites of arachidonic acid. *Am. J. Physiol.* **259**: H1171–H1177.
- Gebremedhin, D., Y. H. Ma, J. R. Falck, R. J. Roman, M. VanRollins, and D. R. Harder. 1992. Mechanism of action of cerebral epoxyeicosatrienoic acids on cerebral arterial smooth muscle. *Am. J. Physiol.* **263**: H519–H525.
- Chen, L., Y. M. Zhu, Y. N. Li, P. Y. Li, D. Wang, Y. Liu, Y. Y. Qu, D. L. Zhu, and Y. L. Zhu. 2017. The 15-LO-1/15-HETE system promotes angiogenesis by upregulating VEGF in ischemic brains. *Neurol. Res.* **39**: 795–802.
- Abdu, E., D. A. Bruun, D. Yang, J. Yang, B. Inceoglu, B. D. Hammock, N. J. Alkayed, and P. J. Lein. 2011. Epoxyeicosatrienoic acids enhance axonal growth in primary sensory and cortical neuronal cell cultures. *J. Neurochem.* **117**: 632–642.
- Hiruma, H., T. Ichikawa, H. Kobayashi, S. Hoka, T. Takenaka, and T. Kawakami. 2000. Prostaglandin E(2) enhances axonal transport and neuritogenesis in cultured mouse dorsal root ganglion neurons. *Neuroscience.* **100**: 885–891.
- Orr, S. K., S. Palumbo, F. Bosetti, H. T. Mount, J. X. Kang, C. E. Greenwood, D. W. Ma, C. N. Serhan, and R. P. Bazinet. 2013. Unesterified docosahexaenoic acid is protective in neuroinflammation. *J. Neurochem.* **127**: 378–393.
- Liu, Y., Y. Wan, Y. Fang, E. Yao, S. Xu, Q. Ning, G. Zhang, W. Wang, X. Huang, and M. Xie. 2016. Epoxyeicosanoid signaling provides multi-target protective effects on neurovascular unit in rats after focal ischemia. *J. Mol. Neurosci.* **58**: 254–265.
- Alkayed, N. J., T. Goyagi, H. D. Joh, J. Klaus, D. R. Harder, R. J. Traystman, and P. D. Hurn. 2002. Neuroprotection and P450 2C11 upregulation after experimental transient ischemic attack. *Stroke.* **33**: 1677–1684.
- Zhang, W., T. Otsuka, N. Sugo, A. Ardeshiri, Y. K. Alhadid, J. J. Iliif, A. E. DeBarber, D. R. Koop, and N. J. Alkayed. 2008. Soluble epoxide hydrolase gene deletion is protective against experimental cerebral ischemia. *Stroke.* **39**: 2073–2078.
- Yuan, L., J. Liu, R. Dong, J. Zhu, C. Tao, R. Zheng, and S. Zhu. 2015. 14,15-Epoxyeicosatrienoic acid promotes production of BDNF from astrocytes and exerts neuroprotective effects during ischemic injury. *Neuropathol. Appl. Neurobiol.* **42**: 607–620.
- Gilroy, D. W., J. Newson, P. Sawmynaden, D. A. Willoughby, and J. D. Croxtall. 2004. A novel role for phospholipase A2 isoforms in the checkpoint control of acute inflammation. *FASEB J.* **18**: 489–498.

41. Deutsch, J., S. I. Rapoport, and A. D. Purdon. 1997. Relation between free fatty acid and acyl-CoA concentrations in rat brain following decapitation. *Neurochem. Res.* **22**: 759–765.
42. Bazán, N. G., Jr. 1970. Effects of ischemia and electroconvulsive shock on free fatty acid pool in the brain. *Biochim. Biophys. Acta.* **218**: 1–10.
43. Rabin, O., M. C. Chang, E. Grange, J. Bell, S. I. Rapoport, J. Deutsch, and A. D. Purdon. 1998. Selective acceleration of arachidonic acid reincorporation into brain membrane phospholipid following transient ischemia in awake gerbil. *J. Neurochem.* **70**: 325–334.
44. Bazan, N. G., T. N. Eady, L. Khoutorova, K. D. Atkins, S. Hong, Y. Lu, C. Zhang, B. Jun, A. Obenaus, G. Fredman, et al. 2012. Novel aspirin-triggered neuroprotectin D1 attenuates cerebral ischemic injury after experimental stroke. *Exp. Neurol.* **236**: 122–130.
45. Marcheselli, V. L., S. Hong, W. J. Lukiw, X. H. Tian, K. Gronert, A. Musto, M. Hardy, J. M. Gimenez, N. Chiang, C. N. Serhan, et al. 2003. Novel docosanoids inhibit brain ischemia-reperfusion-mediated leukocyte infiltration and pro-inflammatory gene expression. *J. Biol. Chem.* **278**: 43807–43817.
46. Wang, L., M. Chen, L. Yuan, Y. Xiang, R. Zheng, and S. Zhu. 2014. 14,15-EET promotes mitochondrial biogenesis and protects cortical neurons against oxygen/glucose deprivation-induced apoptosis. *Biochem. Biophys. Res. Commun.* **450**: 604–609.
47. Kawano, T., J. Anrather, P. Zhou, L. Park, G. Wang, K. A. Fry, A. Kunz, S. Cho, M. Orío, and C. Iadecola. 2006. Prostaglandin E2 EP1 receptors: downstream effectors of COX-2 neurotoxicity. *Nat. Med.* **12**: 225–229.
48. Frankowski, J. C., K. M. DeMars, A. S. Ahmad, K. E. Hawkins, C. Yang, J. L. Leclerc, S. Dore, and E. Candelario-Jalil. 2015. Detrimental role of the EP1 prostanoïd receptor in blood-brain barrier damage following experimental ischemic stroke. *Sci. Rep.* **5**: 17956.
49. Chu, L. S., S. H. Fang, Y. Zhou, G. L. Yu, M. L. Wang, W. P. Zhang, and E. Q. Wei. 2007. Minocycline inhibits 5-lipoxygenase activation and brain inflammation after focal cerebral ischemia in rats. *Acta Pharmacol. Sin.* **28**: 763–772.
50. Rao, A. M., J. F. Hatcher, M. S. Kindy, and R. J. Dempsey. 1999. Arachidonic acid and leukotriene C4: role in transient cerebral ischemia of gerbils. *Neurochem. Res.* **24**: 1225–1232.
51. Wenk, M. R. 2010. Lipidomics: new tools and applications. *Cell.* **143**: 888–895.
52. Yang, J., K. Schmelzer, K. Georgi, and B. D. Hammock. 2009. Quantitative profiling method for oxylipin metabolome by liquid chromatography electrospray ionization tandem mass spectrometry. *Anal. Chem.* **81**: 8085–8093.
53. Wolfer, A. M., M. Gaudin, S. D. Taylor-Robinson, E. Holmes, and J. K. Nicholson. 2015. Development and validation of a high-throughput ultrahigh-performance liquid chromatography-mass spectrometry approach for screening of oxylipins and their precursors. *Anal. Chem.* **87**: 11721–11731.
54. Farias, S. E., M. Basselin, L. Chang, K. A. Heidenreich, S. I. Rapoport, and R. C. Murphy. 2008. Formation of eicosanoids, E2/D2 isoprostanes, and docosanoids following decapitation-induced ischemia, measured in high-energy-microwaved rat brain. *J. Lipid Res.* **49**: 1990–2000.
55. Golovko, M. Y., and E. J. Murphy. 2008. An improved LC-MS/MS procedure for brain prostanoïd analysis using brain fixation with head-focused microwave irradiation and liquid-liquid extraction. *J. Lipid Res.* **49**: 893–902.
56. Murphy, E. J. 2010. Brain fixation for analysis of brain lipid-mediators of signal transduction and brain eicosanoids requires head-focused microwave irradiation: an historical perspective. *Prostaglandins Other Lipid Mediat.* **91**: 63–67.
57. Anton, R. F., C. Wallis, and C. L. Randall. 1983. In vivo regional levels of PGE and thromboxane in mouse brain: effect of decapitation, focused microwave fixation, and indomethacin. *Prostaglandins.* **26**: 421–429.
58. Golovko, M. Y., and E. J. Murphy. 2008. Brain prostanoïd formation is increased by alpha-synuclein gene-ablation during global ischemia. *Neurosci. Lett.* **432**: 243–247.
59. Brose, S. A., S. A. Golovko, and M. Y. Golovko. 2016. Brain 2-arachidonolglycerol levels are dramatically and rapidly increased under acute ischemia-injury which is prevented by microwave irradiation. *Lipids.* **51**: 487–495.
60. Bazinet, R. P., H. J. Lee, C. C. Felder, A. C. Porter, S. I. Rapoport, and T. A. Rosenberger. 2005. Rapid high-energy microwave fixation is required to determine the anandamide (N-arachidonylethanolamine) concentration of rat brain. *Neurochem. Res.* **30**: 597–601.
61. Lust, W. D., J. V. Passonneau, and R. L. Veech. 1973. Cyclic adenosine monophosphate, metabolites, and phosphorylase in neural tissue: a comparison a methods of fixation. *Science.* **181**: 280–282.
62. Schmidt, M. J., D. E. Schmidt, and G. A. Robison. 1971. Cyclic adenosine monophosphate in brain areas: microwave irradiation as a means of tissue fixation. *Science.* **173**: 1142–1143.
63. Stavinoha, W. B., S. T. Weintraub, and A. T. Modak. 1973. The use of microwave heating to inactivate cholinesterase in the rat brain prior to analysis for acetylcholine. *J. Neurochem.* **20**: 361–371.
64. Najarian, T., A. M. Marrache, I. Dumont, P. Hardy, M. H. Beauchamp, X. Hou, K. Peri, F. Gobeil, Jr., D. R. Varma, and S. Chemtob. 2000. Prolonged hypercapnia-evoked cerebral hyperemia via K(+) channel- and prostaglandin E(2)-dependent endothelial nitric oxide synthase induction. *Circ. Res.* **87**: 1149–1156.
65. Walsh, J. L., A. Percival, and P. V. Turner. 2017. Efficacy of blunt force trauma, a novel mechanical cervical dislocation device, and a non-penetrating captive bolt device for on-farm euthanasia of pre-weaned kits, growers, and adult commercial meat rabbits. *Animals (Basel).* **7**: E100.
66. Croston, G., Y. A. Abdel-Aal, S. J. Gee, and B. D. Hammock. 1987. Activation of crude and homogeneous juvenile hormone esterases by organic solvents. *Insect Biochem.* **17**: 1017–1021.
67. Trépanier, M. O., A. Y. Taha, R. L. Mantha, F. A. Giobanu, Q. H. Zeng, G. M. Tchkhartichvili, A. F. Domenichiello, R. P. Bazinet, and W. M. Burnham. 2012. Increases in seizure latencies induced by subcutaneous docosahexaenoic acid are lost at higher doses. *Epilepsy Res.* **99**: 225–232.
68. Taha, A. Y., M. Hennebelle, J. Yang, D. Zamora, S. I. Rapoport, B. D. Hammock, and C. E. Ramsden. 2018. Regulation of rat plasma and cerebral cortex oxylipin concentrations with increasing levels of dietary linoleic acid. *Prostaglandins Leukot. Essent. Fatty Acids.* **138**: 71–80.
69. Xia, J., I. V. Sinelnikov, B. Han, and D. S. Wishart. 2015. MetaboAnalyst 3.0—making metabolomics more meaningful. *Nucleic Acids Res.* **43**: W251–W257.
70. Xia, J., and D. S. Wishart. 2016. Using MetaboAnalyst 3.0 for comprehensive metabolomics data analysis. *Curr. Protoc. Bioinformatics.* **55**: 14.10.1–14.10.91.
71. Trépanier, M. O., M. Eiden, D. Morin-Rivron, R. P. Bazinet, and M. Masoodi. 2017. High-resolution lipidomics coupled with rapid fixation reveals novel ischemia-induced signaling in the rat neuro-lipidome. *J. Neurochem.* **140**: 766–775.
72. Demediuk, P., D. K. Anderson, L. A. Horrocks, and E. D. Means. 1985. Mechanical damage to murine neuronal-enriched cultures during harvesting: effects on free fatty acids, diglycerides, Na⁺,K⁺-ATPase, and lipid peroxidation. *In Vitro Cell. Dev. Biol.* **21**: 569–574.
73. Farias, S. E., K. A. Heidenreich, M. V. Wohlauser, R. C. Murphy, and E. E. Moore. 2011. Lipid mediators in cerebral spinal fluid of traumatic brain injured patients. *J. Trauma.* **71**: 1211–1218.
74. Veech, R. L., R. L. Harris, D. Veloso, and E. H. Veech. 1973. Freeze-blowing: a new technique for the study of brain in vivo. *J. Neurochem.* **20**: 183–188.
75. Ramadan, E., A. O. Rosa, L. Chang, M. Chen, S. I. Rapoport, and M. Basselin. 2010. Extracellular-derived calcium does not initiate in vivo neurotransmission involving docosahexaenoic acid. *J. Lipid Res.* **51**: 2334–2340.
76. Gouveia-Figueira, S., and M. L. Nording. 2015. Validation of a tandem mass spectrometry method using combined extraction of 37 oxylipins and 14 endocannabinoid-related compounds including prostamides from biological matrices. *Prostaglandins Other Lipid Mediat.* **121**: 110–121.